Science Bulletin xxx (2017) xxx–xxx

Contents lists available at ScienceDirect

Science Bulletin

journal homepage: www.elsevier.com/locate/scib

Article

Facile and large-scale synthesis of green-emitting carbon nanodots from aspartame and the applications for ferric ions sensing and cell imaging

Xin Zhang [a], Yun Chen [b], Shou-Nian Ding [a,*]

[a] School of Chemistry and Chemical Engineering, Southeast University, Nanjing 211189, China
[b] Department of Immunology, Nanjing Medical University, Nanjing 210029, China

ARTICLE INFO

Article history:
Received 19 July 2017
Received in revised form 21 August 2017
Accepted 28 August 2017
Available online xxxx

Keywords:
Carbon nanodots
Green-emitting
Aspartame
Ferric ions
Cell imaging
Real sample

ABSTRACT

A facile, economical and green strategy to prepare green-fluorescent nitrogen-doped carbon nanodots (N-CDs) with a quantum yield (QY) of approximately 31.91% has been built up, while aspartame was employed as the carbon–nitrogen source for the first time. The prepared N-CDs exhibited ultrahigh brightness, favorable strong photostability and negligible cytotoxicity. The outstanding optical properties are mainly derived from the their robost composition and steric distribution of the doped nitrogen atoms, which have been characterized detailedly. The obtained N-CDs showed highly selective and sensitive response toward ferric ions (Fe^{3+}) through a fluorescence static quenching process in a wide linear range of 0.005–60 μmol/L. The detection limit was as low as 1.43 nmol/L, allowing the analysis of Fe^{3+} in a very simple method. The excitation-dependent luminescent behavior of the obtained N-CDs guaranteed the multicolor emissive property when they were used in cell imaging. And the application for intracellular Fe^{3+} sensing further verified this novel N-CDs may open more opportunities in biosensor, bioimaging and biological assay.

1. Introduction

Since fluorescent carbon nanodots (CDs) were first discovered during purification process of single-walled carbon nanotubes in 2004 [1], tremendous attention has been drawn to this rising star by virtue of their fascinating features such as excellent optical properties [2], outstanding resistance to photobleaching [3], robust chemical inertness, superior biocompatibility, high water-solubility and so on. Unlike organic dye and semiconductor quantum dots, CDs usually own unique excitation-dependent fluorescence (FL) and break through the limitation of toxic heavy metal element during their formaiton. Thus, CDs show encouraging performance in the in vitro and in vivo bioimaging [4,5], chemical sensors and biosensor [6–8], fluorescent ink [9], light emitting diodes [10], drug delivery [11], medical diagnosis [12], catalysis [13] and so on.

Although the luminescence mechanism of CDs remains controversial, it is believed the FL of CDs roots in the quantum confinement of conjugated π-electrons in the prominent sp^2 carbon network and the surface states [14]. Recently, it is well established that doping foreign heteroatom could endow CDs with tunable fluorescent properties and higher quantum yield (QY) of CDs. Among the heteroatom-doped CDs, nitrogen-doping accounts for the largest proportion in quantity and type, since the comparable atomic size and five valence electrons enable the nitrogen atom to bond with carbon atoms easily and the electron-rich nitrogen atoms could augment the conjugated π-electrons in the carbon framework and thereby improve the QY of CDs [15]. Besides, highly enriched N-doped CDs (N-CDs) offer a convenient and effective platform for heavy metal ion and biomolecule detection because the doped N atoms facilitate the coordination interaction and further enhance the selectivity to the analyte. Up to date, there is still room for us to search for a low-cost precursor acting as both a carbon source and a nitrogen source for the purpose of developing a highly photoluminescent N-CDs.

Till now, most of the reported N-CDs display the strong blue light (λ_{max} = 420–460 nm) under ultraviolet excitation, and their emissions at long wavelength are very weak, that could not meet the requirements for bioimaging. The reasons are the cells and biological tissues commonly emit blue auto-fluorescence which may be overlapped with the FL signal from N-CDs, and ultraviolet excitation may damage the biological matrix [16]. Thus the design and synthesis of the N-CDs with long-wavelength emission remains urgent in this field. Some groups have been engaged in moving the maximum emission light of N-CDs from blue to green, yellow, red, and even near-infrared. For example, Tang's group [17] synthesized a green fluorescent N-CDs using azidoimidizole as a

* Corresponding author.
E-mail address: snding@seu.edu.cn (S.-N. Ding).

http://dx.doi.org/10.1016/j.scib.2017.09.004
2095-9273/

precursor under mild conditions (QY = 7.6%). Xiao and co-workers [18] have reported an "amphiphilic" N-CDs derived from cetylpyridinium chloride with a strong green FL emission to analyze iodine species (QY = 6.8%). Sahu and co-workers [19] used ocimum sanctum as a carbon source to prepare the green-emitting CDs for live cell imaging (QY = 9.3%). Feng and co-workers [20] prepared green fluorescent N-CDs from DL-malic and ethylenediamine by waveoven to quantify guanine (QY = 16.0%). However, most of the reported N-CDs exhibit relatively low QY values (often less than 20%), so it is still a challenge to develop the facile and large-scale preparation of the N-CDs emitting at long wavelength with high QY values.

Iron ions (Fe^{3+}) are considered as the vitalest transition metal ions in life system, involved in diverse biological process including cellular metabolism and homeostasis, oxygen transport, transportation of nerve signals, and so on. Both the deficiency and overdose of Fe^{3+} could induce cellular damages and further cause various diseases like anemia, hepatitis, heart attack, Alzheimer's disease and Parkinson's disease. Moreover, the level of Fe^{3+} is also an essential factor for assessing the water quality. So it is highly demanded to prepare a selective and sensitive chemprobe for Fe^{3+} ions determination. Indeed, a variety of important CDs-based chemprobes have been developed for Fe^{3+} detection [21,22], encouraging us to explore more novel N-CDs selective and sensitive to Fe^{3+} ions.

Herein, we proposed a low-cost and environmental-friendly route to prepare the bright green fluorescent N-CDs by one-pot hydrothermal treatment of aspartame for the first time. Through optimizing the reaction conditions, the as-prepared N-CDs exhibited a high QY (31.91%), much higher than those of the reported green-emitting CDs. The surface composition, chemical state and optical properties of the synthesized CDs were investigated in detail. And a possible formation mechnism was also proposed. The N-CDs exhibited highly efficient fluorescent quenching ability in the presence of Fe^{3+} ions with outstanding sensitivity and selectivity. And this nanoprobe was successfully applied in cell imaging and intracellular Fe^{3+} sensing by virtue of the low toxicity, robust photostability and high QY.

2. Experimental

2.1. Reagents and chemicals

Aspartame ($C_{14}H_{18}N_2O_5$, ≥98.0%) was purchased from Shanghai Dibai Chemical Reagent Co., Ltd. Iron(III) chloride hexahydrate ($Fe_3Cl_6{\cdot}6H_2O$) was obtained from Sinopharm Chemical Reagent Co., Ltd. Cellulose ester dialysis membrane (500 Da MWCO) was purchased from Shanghai Yuanye Bio-Technology Co., Ltd. All other reagents were of analytical grade and were used without further purification. Phosphate buffer solution (PBS, 50 mmol/L) was prepared freshly by varying the ratio of Na_2HPO_4 to NaH_2PO_4. And double distilled water was used throughout. Human gastric carcinoma cells SGC-7901 were purchased from the Type Culture Collection of the Chinese Academy of Sciences (Shanghai, China). RPMI-1640 medium containing 80 U/mL penicillin and 0.08 mg/mL streptomycin, and physiological PBS (pH 7.4) were received from KeyGEN BioTECH Co., Ltd (Nanjing, China). Fetal bovine serum (FBS) and trypsin were obtained from Beyotime Biotechnology Co., Ltd. 3-(4,5-Dimethylthiazol-2-yl)-2,5-diphenyltetra-zolium bromide (MTT) was purchased from Sigma-Aldrich.

2.2. Apparatus

The UV–vis spectra were recorded using a Shimadzu UV-2450 spectrophotometer (Japan). The FL spectra were obtained using a Fluoremax-4 spectrofluorometer (Horiba, USA). The morphology of N-CDs was observed with high resolution transmission electron microscopy (TEM, JEM-2100, JEOL, Japan). Fourier transform infrared (FR-IR) spectrum was collected from a Nicolet 5700 (Thermo Nicolet Corporation, USA) IR spectrometer in the range of 400–4,000 cm^{-1}. The Raman spectrum was collect using Thermo Scientific DXRxi Raman spectrometer (USA) with the excitation wavelength at 532 nm. Powder X-ray diffraction (XRD) data was measured using a Bruker D8 discover X-ray diffractometer (Bruker, Germany). Zeta potential measurements were carried out with Marlvern Zetasizer (Nano ZS, England). All measurements were taken at 25 °C and repeated thrice to calculate the mean value and standard deviation. X-ray photoelectron spectroscopy (XPS) analysis was performed on a Thermo ESCALAB 250 X-ray photoelectron spectrometer (Thermo Scientific, USA). The heights of N-CDs were characterized by atomic force microscopy (AFM) using a Brucker Dimension Edge in the ScanAsyst mode under ambient condition. FL lifetime was measured with FluoroLog 3-TSCPC (Horiba Jobin Yvon Inc., Japan). The absolute photoluminescence quantum yield (PLQY) was tested using a quantum yield accessory, including an integrating sphere which was attached to FluoroLog-3 modular spectrofluorometer (Horiba Jobin Yvon Inc.). MTT assay was measured using a Multiskan GO microplate spectrophotometer (Thermo Fisher Scientific).

2.3. Preparation of the green-emitting N-CDs

The green fluorescent N-CDs were prepared via a hydrothermal method using aspartame as carbon precursor. In brief, aspartame (1.0 g) was added into a mixture of deionized water (25 mL) and ethanol (25 mL), and ultrasonic treatment was performed for 30 min to obtain a homogeneous suspension solution. The well-mixed solution was then transferred into a poly(tetrafluoroethylene)-lined stainless steel autoclave and heated at 185 °C for 4 h. After that, the as-prepared N-CDs were cooled down to room temperature naturally and centrifuged at 10,000 r/min for 20 min to remove the large fragments. The supernatant was further dialyzed against deionized water through a dialysis membrane (500 Da, MWCO) for 24 h. Finally, the resulting N-CDs were dissolved in water as a stock solution (1.5 mg/mL) for further characterization and application.

2.4. Optimizing experimental condition

To obtain better performance for Fe^{3+} detection, the optimization of pH value was performed before assay. In brief, 10 μL of N-CDs dispersion (1.5 mg/mL) was spiked into 50 μL PBS (50 mmol/L) with different pH values, and then 5 L or 30 μL of Fe^{3+} ions (1 mmol/L) was added into the mixture. After that, deionized water was added to control the final volume (500 μL), and the final concentrations of Fe^{3+} are 10 and 60 μmol/L, respectively. The obtained solutions with different pH values were studied by FL spectroscopy with excitation at 410 nm, both the excitation and emission slit widths were 3 nm.

2.5. FL assay of Fe^{3+} ions

The stock solution of Fe^{3+} was freshly prepared from $FeCl_3{\cdot}6H_2O$ using 0.1 mol/L HCl. The fluorometric detection of Fe^{3+} was performed at room temperature in PBS solution (pH 7.0). In a typical run, 10 μL of N-CDs dispersion (1.5 mg/mL) was added into 50 μL PBS solution (50 mmol/L), followed by the addition of Fe^{3+} standard with different concentrations. The final volume of the mixture was adjusted to 500 μL with deionized water, and then the system was shaken gently by a vortex mixer for 2 min. After incubation for 15 min at room temperature, the FL emission intensity of the

Please cite this article in press as: Zhang X et al. Facile and large-scale synthesis of green-emitting carbon nanodots from aspartame and the applications for ferric ions sensing and cell imaging. Sci Bull (2017), http://dx.doi.org/10.1016/j.scib.2017.09.004

sample was measured at the excitation wavelength of 410 nm. The quenching efficiencies of Fe^{3+} toward N-CDs were calculated according to the equation: quenching efficiency = $(FL_0 - FL)/FL_0$, where FL_0 and FL represent the FL intensities in the absence and presence of Fe^{3+}, respectively. The selectivity of the N-CDs toward Fe^{3+} was evaluated by adding other competitive metal ions and anions in the similar way.

2.6. Detection of Fe^{3+} ions in real samples

To evaluate the potential application of the fluorescent N-CDs in biological samples and environmental samples, the Fe^{3+} determinations were also conducted in urine sample, serum sample and lake water. Human urine and serum samples were obtained from Southeast University Affiliated Zhongda Hospital (Nanjing, China). Lake water was collected from Jiulong Lake in Nanjing (China). The urine sample was 100-fold diluted with PBS (5 mmol/L, pH 7.0) before analysis. And the serum sample was centrifuged at 3,000 r/min for 15 min to remove the protein. Considering iron may exist as ferrous in serum, 5 μL of 3% H_2O_2 solution was added into the supernatant to oxidize Fe^{2+} to Fe^{3+}. The obtained sample was then diluted with 5 mmol/L PBS by 100-fold for subsequent analysis. For the lake water sample, centrifugation at 10,000 r/min for 15 min and filtration with a syringe filter (0.45 μm) were performed to remove the impurities. The recovery test was performed by spiking Fe^{3+} standards into the samples according to the standard addition method.

2.7. Cytotoxicity test

Human gastric carcinoma cells SGC-7901 were used as model cells to investigate the cytotoxicity and cellular imaging capacity of N-CDs. The N-CDs solution was sterilized by filtration with a sterile syringe filter (0.22 μm). The cytotoxicity of N-CDs was determined by a standard MTT assay. Briefly, SGC-7901 cells were seeded into a 96-well plate at a density of 5×10^3 cells per well in RPMI-1640 culture medium supplemented with 10% FBS. The cells were cultured in a humidified incubator with 5% CO_2 at 37 °C for 24 h first to allow the cell adhesion. Then the cells were washed with PBS twice and cultured with fresh culture medium containing N-CDs of various concentrations (0–400 μg/mL) for another 24 h. Six parallel measurements were conducted for each concentration, and cells without treatment with N-CDs were set as a control. Afterwards, the culture medium in each well was discarded and the wells were washed with PBS. Then, 20 μL of MTT (5 mg/mL in PBS) and 130 μL of fresh culture medium were added into each well. After a further incubation for 4 h, the culture medium with MTT was removed and 100 μL of DMSO was added into each well to dissolve formazan crystal. After shaking for 10 min in dark, the optical density (OD) of the resultant mixture in each well at 570 nm was recorded by the microplate spectrophotometer. The cell viability was derived according to the equation of cell viability (%) = $(OD_{treated}/OD_{control}) \times 100\%$, where $OD_{treated}$ refers to the cells treated with N-CDs and $OD_{control}$ represents the cells incubated with culture medium only. The final results were obtained from three experiments.

2.8. Multicolor cellular imaging

For *in vitro* cell imaging investigation, SGC-7901 cells (2×10^4) were grown on glass coverslips placed at the bottom of 24-well plate and incubated for 24 h for cell adhesion. The N-CDs solution was also sterilized by filtration with a sterile syringe filter (0.22 μm). Subsequently, the cells were rinsed with PBS twice to remove the non-adherent cells, followed by incubation with 1 mL fresh culture medium containing 300 μg/mL N-CDs for 8 h. Thereafter, the cells were washed with PBS twice to remove the extracellular N-CDs, fixed with 4.0% paraformaldehyde for 15 min immediately, and then rinsed with PBS again. The cell imaging was acquired using a confocal laser scanning microscopy (Zeiss LSM 710, Carl Zeiss AG, Germany).

In addition, the N-CDs loaded cells were treated with different concentrations of Fe^{3+} in 1 mL PBS for 10 min and then washed with PBS twice. Finally, the FL images were collected in the same condition.

3. Results and discussion

3.1. Synthesis of the green fluorescent N-CDs

As shown in Scheme 1, the green-emissive N-CDs were synthesized via a simple hydrothermal treatment using aspartame as carbon precursor and ethanol as stabilizer. Herein, aspartame was carefully chosen for the following reasons. On the one hand, aspartame, as a kind of easily available and low-cost sweetener, is made from the aspartic acid/phenylalanine dipeptide. So, there is no toxic agent in the whole synthesis process, which makes the reaction eco-friendly. On the other hand, the source molecule itself includes one carboxylic group and one amino group, and thus intermolecular dehydration and hydrothermal polymerization may be easily achieved at the initial stage. Over time, carbonaceous nuclei forms through the cross-linked polymerization and the size grows gradually at the expense of aspartame. At the same time, the heteroatoms, N and O, incorporate into the carbon matrix and bring in defect sites, which could also control the sp^2 domain [23]. In addition, the two functional groups, carboxylic group and amino group, may be also transferred from aspartame to the N-CDs, leading to the in situ functionalization and excellent dispersion in water [24]. To obtain the best FL performance, a series of synthetic parameters were optimized before application, such as source concentration, the volume of ethanol and reaction time. As can be seen in Fig. S1a (online), the maximum emission intensity of N-CDs at 509 nm increased with the increase of aspartame concentration from 5 to 20 mg/mL, and then decreased when the concentration was higher than 20 mg/mL. Thus 20 mg/mL was chosen as the optimal concentration of the precursor. The ethanol volume was found to greatly affect the FL emission intensity of the N-CDs (Fig. S1b online). The FL intensity increased to a maximum value when the ethanol volume was 25 mL, suggesting the involvement of ethanol in the synthesis of N-CDs. Fig. S1c (online) displays that the FL intensity increased with the reaction time and reached a plateau at 4 h, indicating structurally rigid planes with incorporated N/O atoms may form at this time and the stable carbon dots with the highest FL intensity were obtained.

3.2. Structure and composition of the as-prepared N-CDs

The morphology and size of the green-emitting N-CDs were observed by TEM. As shown in Fig. 1a, the obtained N-CDs were spherical in shape and well dispersed in aqueous medium without apparent aggregation. Fig. 1b shows the corresponding size distribution obtained by counting 111 particles in TEM image. The sizes of N-CDs were mainly distributed in the range from 1.5 to 4.5 nm with an average diameter of 3.0 nm, further demonstrating the N-CDs have good monodispersity.

XRD pattern of N-CDs shows a broad diffraction peak at $2\theta = 23.0°$, attributed to the (0 0 2) plane of a graphitic structure (Fig. 1c). And the corresponding interlayer spacing is about 0.38 nm, larger than the interlayer distance of graphite (0.34 nm) [25], further implying there are abundant functional groups in the core or on the surface [26].

Please cite this article in press as: Zhang X et al. Facile and large-scale synthesis of green-emitting carbon nanodots from aspartame and the applications for ferric ions sensing and cell imaging. Sci Bull (2017), http://dx.doi.org/10.1016/j.scib.2017.09.004

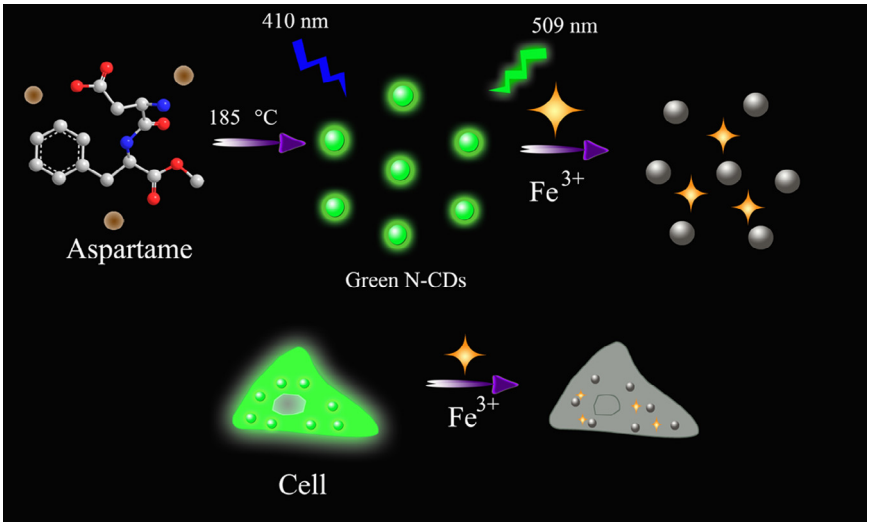

Scheme 1. (Color online) Schematic diagram of the preparation of the green-emitting N-CDs and Fe^{3+} detection.

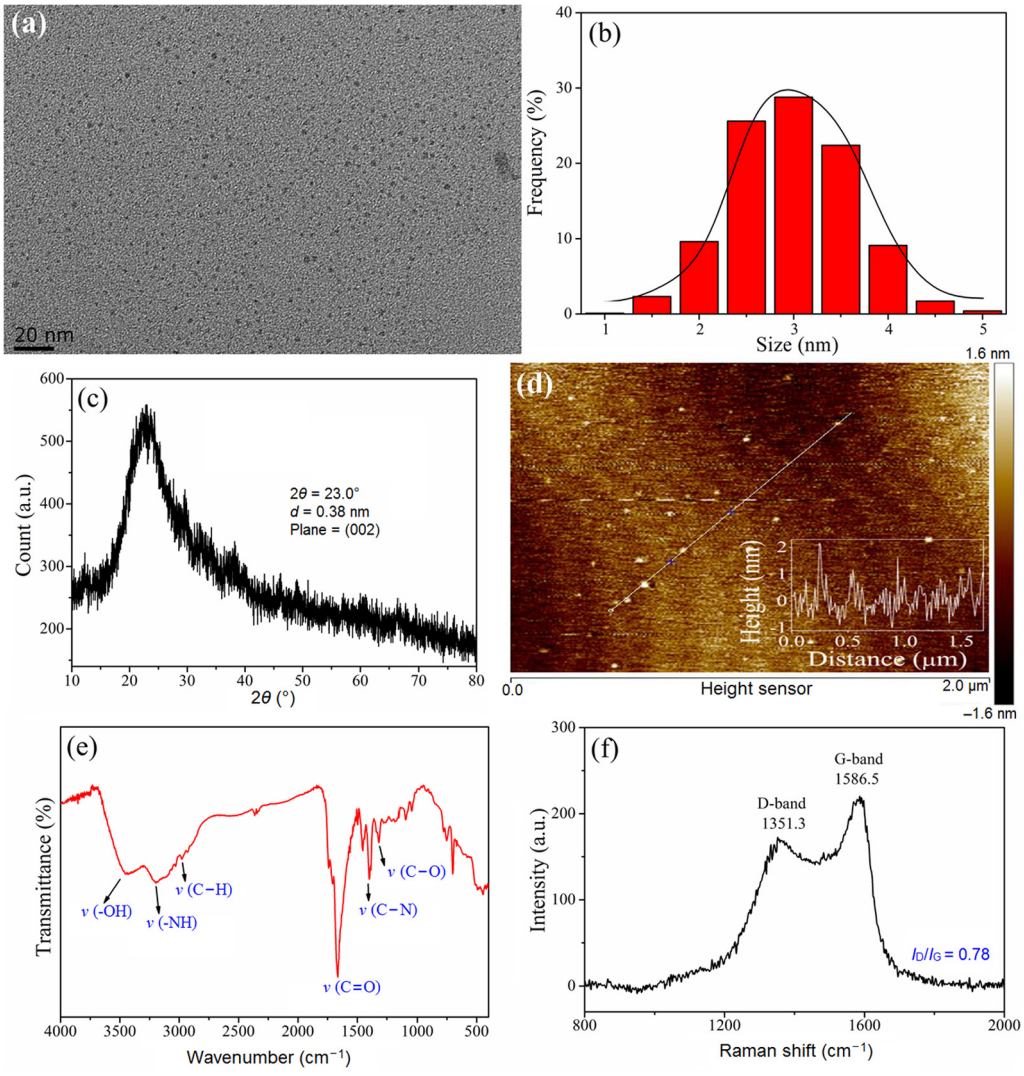

Fig. 1. (Color online) Morphological and structural characterization of as-prepared N-CDs. (a) TEM image, (b) particle size distribution, (c) XRD pattern, (d) AFM image, (e) FT-IR spectrum and (f) Raman spectrum of N-CDs. The inset in (d) shows the corresponding height profile along the line.

Please cite this article in press as: Zhang X et al. Facile and large-scale synthesis of green-emitting carbon nanodots from aspartame and the applications for ferric ions sensing and cell imaging. Sci Bull (2017), http://dx.doi.org/10.1016/j.scib.2017.09.004

The thickness and height distribution of N-CDs were characterized by AFM (Fig. 1d). The topographic heights were mainly in the range of 1.2–2.2 nm, suggesting most of the N-CDs comprise 3–6 layers of graphene sheets [14].

The bonding manner and functional groups of the N-CDs were initially analyzed using FT-IR spectroscopy. As displayed in Fig. 1e, the broad absorption bands at 3,455 and 3,205 cm^{-1} can be ascribed to the stretching vibrations of O—H and N—H, respectively [27,28]. The peaks at 3,029–2,927 cm^{-1} are related to the C—H stretching vibration mode of aromatic rings [29]. And the sharp peak at 1,664 cm^{-1} corresponds to C=O stretching vibrations of the carboxylic group [30]. Two characteristic peaks at 1,399 and 1,317 cm^{-1} are attributed to C—N and C—O stretching vibrations, respectively [31]. In addition, the peaks in the range of 900−650 cm^{-1} are associated with out-of-plane bending vibrations of O—H and N—H. From these results, we can deduce that large number of hydroxyl groups, amino groups and carboxylic groups exist on the surface of the N-CDs, and these functional groups may improve the hydrophilicity and stability.

The Raman spectrum of the synthesized N-CDs (Fig. 1f) reveals two distinct peaks centering at 1,351.3 and 1,586 cm^{-1}, corresponding to a disordered D band and crystalline G band, respectively. The G band corresponds to the E_{2g} mode of graphite, related to the in-plane vibration of sp^2-hybridized carbon atoms in the graphitic sheet [32]. And the D band is assignable to the vibrations of sp^3-hybridized carbon atoms with dangling bonds, reflecting the defects in the graphitic sheet. The intensity ratio of D band to G band (I_D/I_G) was 0.78, indicating the obtained N-CDs have a graphitic structure with a plenty of structural defects [33]. The surface defects were mainly caused by surface oxidation and nitrogen doping.

To identify the surface composition and chemical state, the obtained N-CDs were further characterized by XPS. The survey spectrum (Fig. 2a) exhibits three characteristic peaks at 285, 401 and 532 eV, which are assigned to C 1s, N 1s, and O 1s peaks, respectively. The XPS quantitative analysis suggests the N-CDs are composed of C (68.0%), N (10.4%) and O (21.6%). It is well established nitrogen doping could facilitate the surface passivation of carbon materials [34]. The high-resolution C 1s spectrum of the N-CDs (Fig. 2b) exhibits five peaks at 284.5, 285.3, 286.5, 287.6 and 291.1 eV, corresponding to C—C/C=C, C—N [35], C—O [3,36], C=N/C=O [37] and O—C=O bonds [38], respectively. The presences of C=C, C—N and C=N peaks confirm the graphitic structure of the N-CDs contains heterocyclic aromatic moieties. Further, the N 1s spectrum (Fig. 2c) mainly consists of three peaks centering at 398.9, 399.8 and 401.6 eV, ascribed to graphitic N [39], pyridinic N/pyrrolic N [40] and N—H bond [41], respectively, demonstrating the nitrogen element on the surface of N-CDs exists in forms of polycyclic heterocycles and amino groups. The O 1s spectrum (Fig. 2d) was deconvoluted into three components located at 531.1, 531.9 and 533.3 eV, which are associated with C=O [42], C—OH [38] and C—O—C groups [43], respectively. Consistent with the FT-IR results, XPS results confirm the existence of the polycyclic heterocycles and abundant hydrophilic groups on surface of N-CDs (e.g., hydroxyl, amino and carboxylic groups).

To further investigate the surface information on N-CDs, zeta potential measurements were carried out. As shown in Fig. S2 (online), the isoelectric point (pI) of N-CDs is 5.0, higher than that of undoped CDs (3.4) in previous report [41]. It could be deduced that N-doping may form nitrogen-containing functional groups (like -NH_2) on their surfaces and the ionization of these groups would lead to the higher pI. It also could be observed that the N-CDs have a potential of −14.3 mV in PBS (pH 7.0), implying the negatively charged carboxyl groups predominate on their surfaces. And the electrostatic repulsion between the N-CDs ensured the

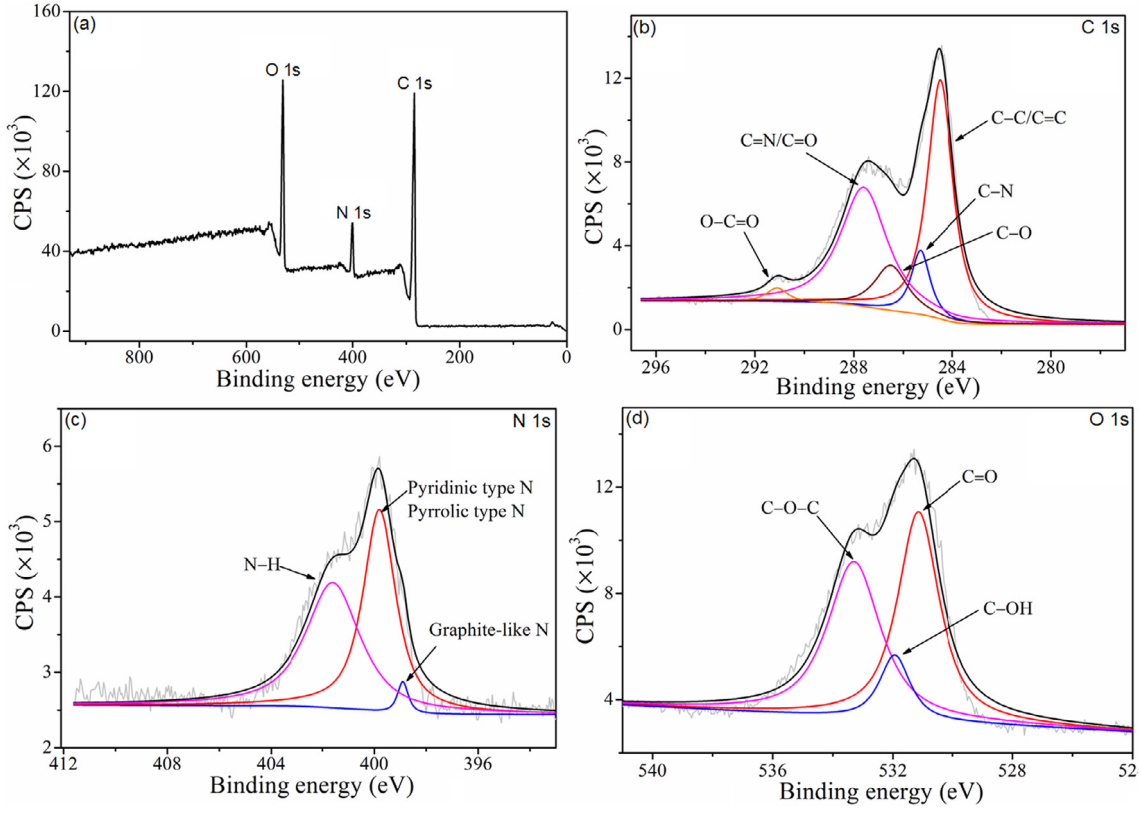

Fig. 2. (Color online) XPS survey spectrum (a), high-resolution C 1s (b), N 1s (c) and O 1s (d) XPS spectra of the obtained N-CDs.

Please cite this article in press as: Zhang X et al. Facile and large-scale synthesis of green-emitting carbon nanodots from aspartame and the applications for ferric ions sensing and cell imaging. Sci Bull (2017), http://dx.doi.org/10.1016/j.scib.2017.09.004

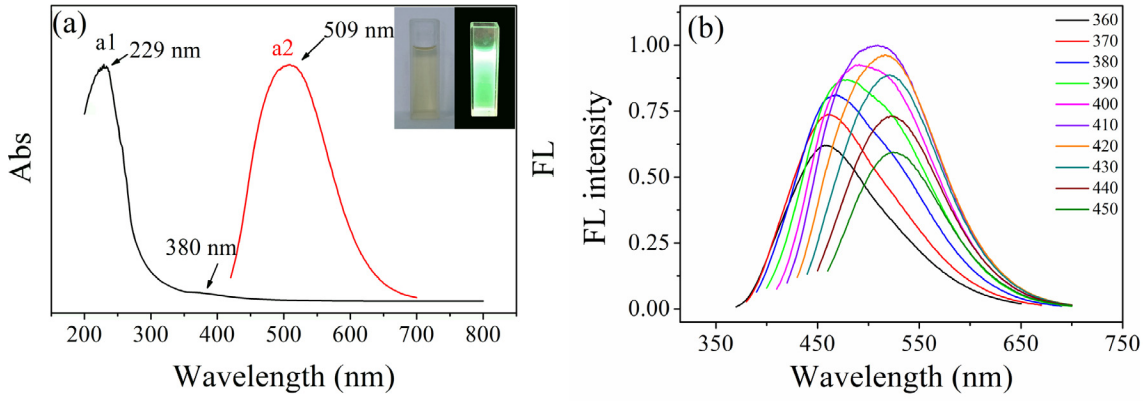

Fig. 3. (Color online) Optical properties of N-CDs. (a) UV–vis absorption (a1) and FL emission (a2, λ_{ex} = 410 nm) of the N-CDs. Inset: Photographs under daylight and UV light (365 nm). (b) FL emission spectrum of the N-CDs at different excitation wavelengths from 360 to 450 nm, both the excitation and emission slit widths were 3 nm.

excellent storage stability. The obtained N-CDs were stable for 4 months without any agglomeration.

3.3. Optical properties and stability of the as-prepared N-CDs

The optical properties of the obtained N-CDs were investigated by UV–vis absorption and FL emission spectra. The UV–vis spectrum (Fig. 3a) display a strong absorption peak at 229 nm and a weak shoulder peak around 380 nm (curve a1). The peak at 229 nm is attributed to π-π^* transition of C=C and C=N bonds [44], confirming the polycyclic heterocyclic structure of the graphene layer in N-CDs. The shoulder peak at 380 nm corresponds to the n-π^* transition of the carbonyl groups on the surface of N-CDs. The FL emission spectrum (curve a2) shows that the maximum emission wavelength located at 509 nm when the N-CDs solution was excited at 410 nm. And the light yellow aqueous solution of N-CDs emitted very bright green luminescence under UV light (365 nm), which could be clearly seen in the inset of Fig. 3a.

Similar with most luminescent CDs [20,45], the N-CDs derived from aspartame also exhibited an excitation-dependent photoluminescence behavior. As illustrated in Fig. 3b, the maximum emission wavelength of the N-CDs solution shifted from 459 to 524 nm when excited from 360 to 450 nm, and the FL intensity increased gradually and then decreased, revealing the multicolor properties. This observation may be due to the nonuniformity of the grain size and different surface energy traps caused by surface groups [10]. The different kinds of surface energy traps are associated with different energy levels, resulting in a broad and excitation-dependent emission spectrum correspondingly. Besides, the PLQY of the obtained N-CDs is as high as 31.91% (excited at 410 nm), higher than most of the reported green-emitting CDs and strong enough for imaging applications [17–20].

To evaluate the stability of the N-CDs toward complex environment, the FL properties of N-CDs aqueous solution under various conditions were examined. The influence of pH value on the FL property was first assessed and shown in Fig. S3a (online). The FL emission peak did not shift with the variation of pH value, but the FL intensity was affected to a certain degree. The N-CDs showed a strong and stable FL intensity in a broad pH range (4–10). Under very acidic or alkaline conditions, the FL intensities were relatively low, probably due to the change in the surface charge of N-CDs, associated with protonation/deprotonation process of amine groups and CN units on the surface or edge [46]. This speculation is supported by zeta potential analysis. The impact of ionic strength on the stability of N-CDs was also investigated by measuring the FL intensities of the N-CDs in different concentrations of NaCl. As depicted in Fig. S3b (online), only a slight change in FL intensity was observed even though the NaCl concentration was as high as 1.0 mol/L, indicating that the N-CDs have good salt tolerance and may be employed in biological system. In addition, less than 3% decline in FL intensity was obtained when the sample was stored for 60 days (Fig. S3c online). And the N-CDs solution was still homogeneous phase without any floater and precipitation. All these results confirm that this stable N-CDs may be valuable for real applications in bioimaging and bioanalysis.

3.4. Optimizing experimental conditions

The feasibility of employing N-CDs as a probe for metal ions was investigated by FL measurement. In a preliminary study, it was found that the Fe^{3+} exerted a strong FL quenching effect on N-CDs (Fig. S4a online). The inset displays the N-CDs solution before and after adding 160 μmol/L Fe^{3+} ions under UV lamp irradiation (365 nm), and the Fe^{3+} recognition could be directly monitored by naked eyes. Fe^{3+} ions play a crucial role in cellular metabolism and oxygen transport, being of great significance in biological systems. Thus we further explored the capacity of the N-CDs for Fe^{3+} detection.

The pH of the reaction solution is a determining factor for the detection sensitivity, so optimization experiment was conducted before the assay. Fig. S4b (online) displays the FL responses of the N-CDs toward 10 and 60 μmol/L Fe^{3+} at different pH values. The N-CDs exhibited the strong FL intensity and robust chemical stability when the pH values were in the range of 5.0–9.0. But the quenching efficiencies for Fe^{3+} were different at various pH values and the optimal pH value was found to be 7.0. This is mainly because the protonation process of the -NH_2 groups may occur under acidic conditions, inhibiting the coordination of Fe^{3+} ions to the N-CDs via electrostatic repulsion, suppressing the formation of Fe^{3+}-N-CDs complex and thereby resulting in incomplete FL quenching. On the other hand, Fe^{3+} may precipitate in form of ferric hydroxide under alkaline condition, leading to the low FL quenching effect. Therefore, PBS (pH 7.0) was selected as the buffer solution for the assay of Fe^{3+} ion using N-CDs as a fluorescent probe.

3.5. Fe^{3+} detection using the N-CDs as fluorescent probe

For a sensitivity study, FL changes were recorded after addition of Fe^{3+} ions for a fixed time of 17 min so as to ensure the reliability and reproducibility of the sensing response. Fig. 4a shows the FL spectra of the N-CDs solution upon addition of Fe^{3+} ions at the concentration from 0 to 200 μmol/L. A gradual decrease in FL intensity at 509 nm was observed and the green FL of N-CDs was quenched

Please cite this article in press as: Zhang X et al. Facile and large-scale synthesis of green-emitting carbon nanodots from aspartame and the applications for ferric ions sensing and cell imaging. Sci Bull (2017), http://dx.doi.org/10.1016/j.scib.2017.09.004

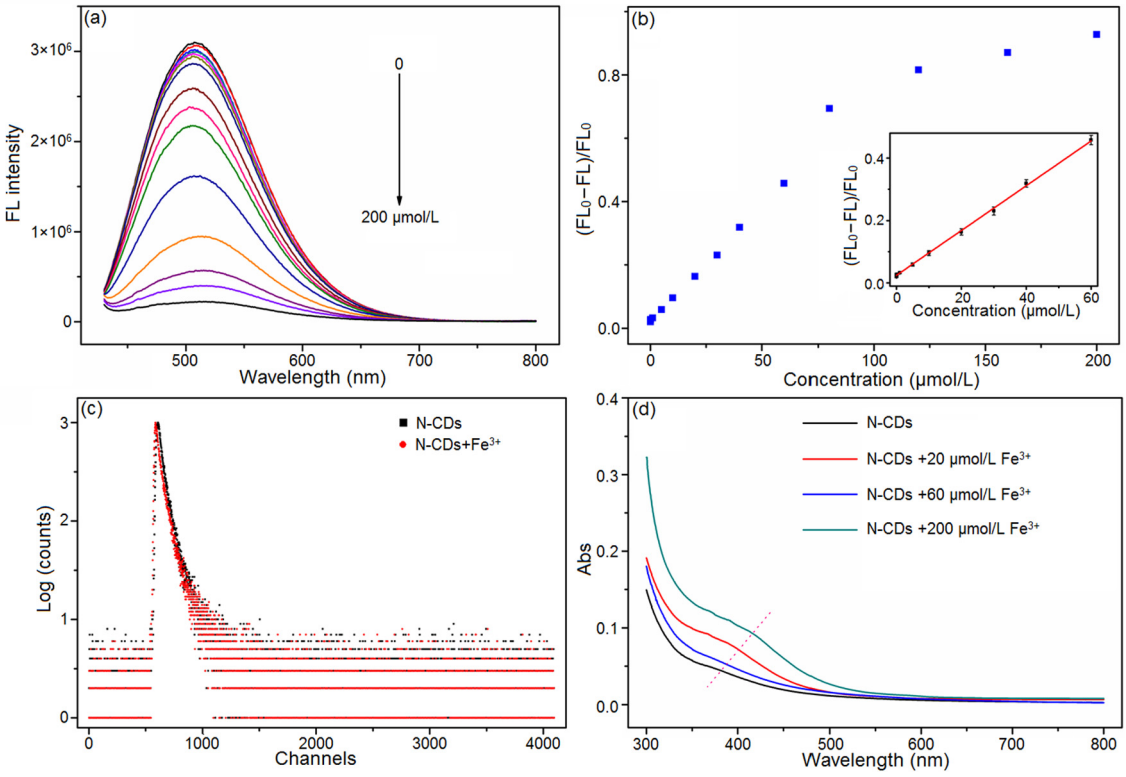

Fig. 4. (Color online) Quenching effect on Fe^{3+} ions. (a) FL emission spectra of N-CDs (30 μg/mL) in the presence of different concentrations of Fe^{3+} ions (0, 0.005, 0.01, 0.1, 1, 5, 10, 20, 30, 40, 60, 80, 120, 160 and 200 μmol/L, top to bottom, λ_{ex} = 410 nm). (b) Plots of the value of $[(FL_0 - FL)/FL_0]$ versus the concentrations of Fe^{3+} ions. Inset: the linear relationship between $[(FL_0 - FL)/FL_0]$ and Fe^{3+} concentration. The error bars represent the standard deviation of three measurements. (c) FL decay of N-CDs in the absence and presence of Fe^{3+} ions (100 μmol/L). (d) UV–vis absorption of N-CDs at various concentrations of ions.

completely upon adding 200 μmol/L Fe^{3+}, revealing the sensing system is sensitive to Fe^{3+} ion concentration. And the quenching efficiency $(FL_0-FL)/FL_0$ displayed a good linear relationship versus Fe^{3+} concentration in the range of 0.005–60 μmol/L (inset of Fig. 4b) with a correlation coefficient (R^2) of 0.995, where FL_0 and FL represent the FL intensities at 509 nm in the absence and presence of Fe^{3+}, respectively. A detection limit of 1.43 nmol/L was estimated according to the signal-to-noise ratio of 3, which is much lower than the threshold value of Fe^{3+} ions in drinking water (0.3 ppm, ~5.36 μmol/L) as regulated by the World Health Organization (WHO) and U.S. Environmental Protection Agency (EPA). Furthermore, we made a comparative work on the performance of the proposed fluorescent probe with other probes, including CDs from different carbon source and organic compound (shown in Table S1 online). It could be found that our probe presents a relatively wide linear range with a low detection limit, confirming the N-CDs can be used as a robust FL probe for Fe^{3+} ions with satisfactory sensitivity and simplicity.

3.6. Possible mechanism of the FL response of N-CDs to Fe^{3+} ions

To gain an insight into the FL quenching mechanism provoked by Fe^{3+}, FL decay and UV–vis absorption of the N-CDs in the absence and presence of Fe^{3+} were measured. FL decay was performed by time-correlated single-photon counting (TCSPC) technique and the decay curves were fitted with a biexponential function. Two time-resolved decay lifetimes (τ_1 and τ_2) were assessed by FL decay curves and shown in Table S2 (online), where A_1 and A_2 represent the fractional contributions of τ_1 and τ_2, respectively. As depicted in Fig. 4c, no discernable change in the decay curve was found after the addition of Fe^{3+}. Meanwhile, the average lifetime of N-CDs was calculated as 2.64 ns. Upon addition of Fe^{3+} ions to the N-CDs solution, the average lifetime was about 2.21 ns. The nearly constant FL lifetime reveals the quenching of N-CDs by Fe^{3+} ions obeys a simple static quenching mechanism. Static quenching takes place when the FL material forms a complex in the ground state with the quencher [1]. Fe^{3+} is known to be a strong Lewis acid due to its half-filled 3d orbital, which has a strong affinity for electron-rich groups (O/N-containing groups). It has been confirmed by FT-IR, XPS and zeta potential results that large numbers of -NH_2, -OH, -COOH groups exist on the surfaces of the fluorescent N-CDs. Therefore, upon gradual addition of Fe^{3+} to N-CDs solution, the electron may be transferred from the electron-rich groups of N-CDs and partly donated to Fe^{3+} ions. Namely, the FL quenching behavior is based on nonradiative electron transfer process. In addition, as discussed in previous literatures [47,48], Fe^{3+} could react with the -NH_2, -OH, -COOH groups on the surfaces of N-CDs, induce the formation of nonfluorescent Fe^{3+}/N-CDs metal complexes, and thereby give rise to the diminished luminescent characteristics.

In addition, static quenching often accompanies with the change in absorption peak because the formed nonfluorescent complex possesses its unique absorption spectrum. As shown in Fig. 4d, the shoulder peak of N-CDs shifted from 380 to 416 nm upon the addition of Fe^{3+} ions, further implying the FL response of N-CDs to Fe^{3+} ions follows the static quenching mechanism.

3.7. Selectivity of the green-emissive N-CDs probe

The selectivity of the N-CDs probe for Fe^{3+} detection was tested via interference experiment. Under the optimal conditions, FL intensity changes of the N-CDs in presence of representative metal ions and anions (i.e., Mg^{2+}, Cd^{2+}, Zn^{2+}, Hg^{2+}, Au^{3+}, Ni^{2+}, Mn^{2+}, Cu^{2+}, K^+, Na^+, Sn^{4+}, Sr^{2+}, Sn^{2+}, Ca^{2+}, Fe^{2+}, Co^{2+}, Eu^{3+}, Ag^+, Pb^{2+}, Cr^{3+}, NO_2^-,

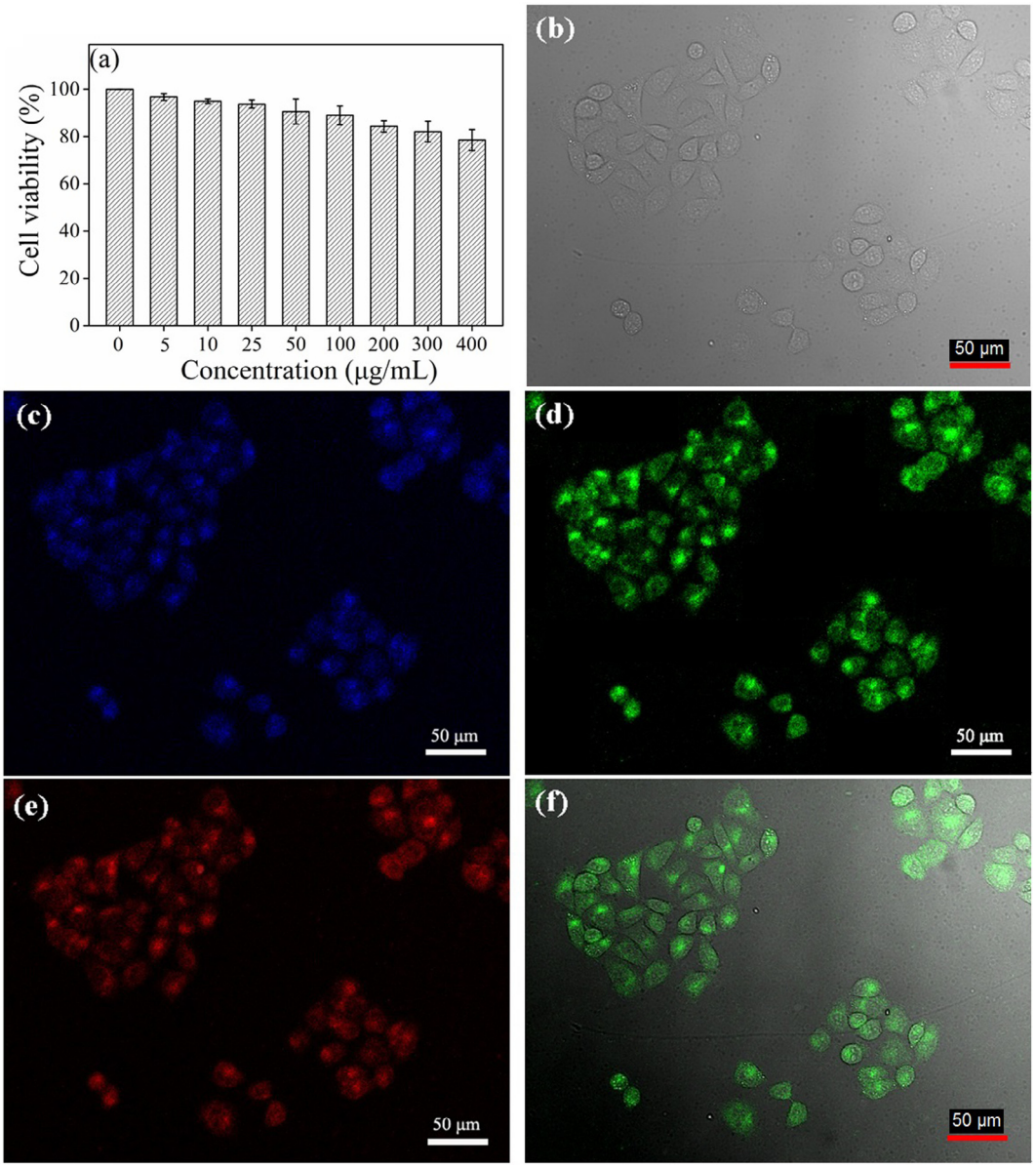

Fig. 5. Cell imaging of N-CDs. (a) Viability (%) of SGC-7901 cells after incubation with different doses of N-CDs for 24 h. Confocal fluorescence images of SGC-7901 cells after incubation with N-CDs for 8 h under bright field (b), taken at $\lambda_{ex}/\lambda_{em}$ of 405/420–480 nm (c), 405/500–560 nm (d) and 555/600–700 nm (e), and the merged image (f) of b and d.

Cl^-, I^-, $H_2PO_4^-$, ClO_4^-, SO_4^{2-}) were studied. As shown in Fig. S5 (online), the addition of Fe^{3+} led to an evident quenching effect, and other metal ions or anions exhibited negligible effects. These observations may be attributed to the stronger binding affinity and quicker chelating kinetics of the Fe^{3+} ions with the N/O functional groups on the N-CDs surfaces than other metal ions and anions [49]. The outstanding selectivity of the N-CDs for Fe^{3+} ions is extremely valuable for it implies their potential use in real sample.

3.8. Real samples

To evaluate the reliability of the developed method and its potential application in real samples, recovery tests were conducted according to the standard addition method in three samples, human urine, serum and lake water. As shown in Table S3 (online), after the addition of Fe^{3+} standards into the sample, the recovery results ranged from 98.5% to 105.0%, indicating the high analytical precision of the current method. The results also demonstrate the potential interference in the sample matrix was hardly a threat to Fe^{3+} detection. And all RSD values were less than 4.43%. These results further confirm the reliability and feasibility of the N-CDs probes for monitoring the Fe^{3+} in real samples.

3.9. Cytotoxicity and cell imaging capacity of the as-prepared N-CDs

Cytotoxicity is an indispensable factor that requires careful investigation prior to subsequent biological applications. The cytotoxicity of the potential fluorescent nanoprobes was assessed by calculating the viability from MTT results and conducting the morphological analysis. Fig. 5a illustrates a dose-dependent characteristic of the cell viability. And the viability of SGC-7901 cells still remained above 82.2% upon incubation with the N-CDs at a high dose of 300 μg/mL for 24 h. In addition, the bright field image exhibits the cells maintained their normal morphology after incubation with the N-CDs for 8 h (Fig. 5b). Compared with the cells untreated

Please cite this article in press as: Zhang X et al. Facile and large-scale synthesis of green-emitting carbon nanodots from aspartame and the applications for ferric ions sensing and cell imaging. Sci Bull (2017), http://dx.doi.org/10.1016/j.scib.2017.09.004

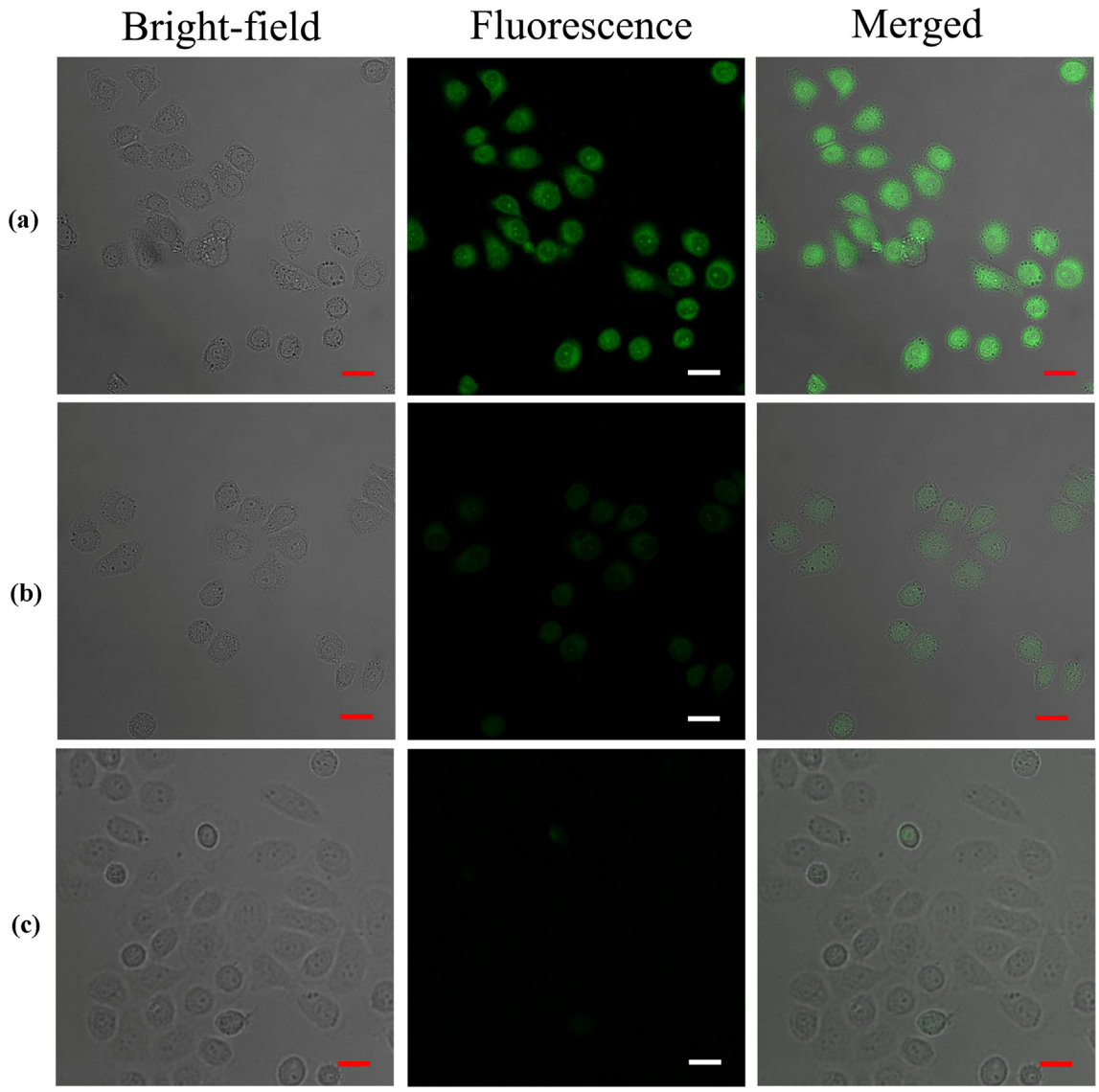

Fig. 6. (Color online) Confocal fluorescence images of N-CDs-loaded SGC-7901 cells without Fe^{3+} ions (a); treated with 100 μmol/L Fe^{3+} ions (b) and 200 μmol/L Fe^{3+} ions (c). Fluorescence images were excited at 405 nm and collected in the range of 500–560 nm. Scale bar: 20 μm.

with N-CD (Fig. S6a online), no discernable change was found in their fusiform shape and good adherence. These results confirm that the fluorescent N-CDs possess excellent biocompatibility with low cytotoxicity, which is advantageous to the application in cell imaging and sensing.

The potential application of the as-prepared N-CDs as a fluorescent probe for in vitro imaging was demonstrated by labeling the SGC-7901 cells. As can be seen from Fig. 5c–e, the cells treated with N-CDs exhibited bright blue, green and red emissions at the corresponding excitation wavelengths, whereas no obvious emission was observed from the cells in absence of N-CDs (Fig. S6b online). It also could be found in the merged image that the region of the green emission matches well with the locations of the cells under the bright field, proving that a large number of N-CDs were internalized into the cells (Fig. 5f). Similar with previous reports [49], the fluorescent emission dispersed unevenly in each cell, mainly because the CDs without specific functionalization label the cell membrane and cytoplasm basically through passive endocytosis without entry into the nuclei [50,51]. The multicolor emissive property is preferential for a broad-spectrum FL probe could give us much space to select the wavelength for observation [52].

3.10. Intracellular imaging of Fe^{3+} ions

Encouraged by above-mentioned high sensitivity to Fe^{3+} ions, we further determined the exogenous Fe^{3+} ions in live cells using SGC-7901 cells as a model cell line. As displayed in Fig. 6a, bright green FL emission was found within intracellular region. When the N-CDs-loaded cells were treated with Fe^{3+} ions, the FL brightness decreased gradually with the increase of Fe^{3+} concentration (Fig. 6b and c). These results indicated the N-CDs are cell permeable and capable of imaging Fe^{3+} in live cells.

4. Conclusions

In summary, an economical and facile method has been successfully developed for preparing the green-emitting nitrogen-doped carbon nanodots (N-CDs) through one-pot hydrothermal treatment of aspartame for the first time. The obtained N-CDs possessed strong luminescence at 509 nm with a relatively high absolute quantum yield of 31.91%. Different from other blue-emitting CDs, our N-CDs could minimize the background fluorescence from cell or tissue. The as-prepared N-CDs displayed outstanding salt

Please cite this article in press as: Zhang X et al. Facile and large-scale synthesis of green-emitting carbon nanodots from aspartame and the applications for ferric ions sensing and cell imaging. Sci Bull (2017), http://dx.doi.org/10.1016/j.scib.2017.09.004

tolerance, admirable stability, excellent sensitivity and selectivity toward ferric (Fe^{3+}) ions. By spectral and fluorescence decay investigation, static quenching mechnism between the label-free N-CDs and Fe^{3+} ions was proposed. Meanwhile, the low cytotoxicity and good cell permeability of the N-CDs enable the cell imaging and intracellular ferric ions analysis, suggesting the promising application in bioanalysis. In the future work, these CDs would be applied for in vivo imaging and biomedical research.

Conflict of interest

The authors declare that they have no conflict of interest.

Acknowledgments

This work was supported by the National Natural Science Foundation of China (21575022, 21535003), the National High Technology Research and Development Program of China (2015AA020502), the Fundamental Research Funds for the Central Universities (2242016K41055), Qing Lan Project and the Priority Academic Program Development of Jiangsu Higher Education Institutions (1107047002).

Appendix A. Supplementary data

Supplementary data associated with this article can be found, in the online version, at http://dx.doi.org/10.1016/j.scib.2017.09.004.

References

[1] Shi L, Li Y, Li X, et al. Controllable synthesis of green and blue fluorescent carbon nanodots for pH and Cu^{2+} sensing in living cells. Biosens. Bioelectron 2016;77:598–602.
[2] Mei Q, Chen J, Zhao J, et al. Atomic oxygen tailored graphene oxide nanosheets emissions for multicolor cellular imaging. ACS Appl. Mater. Interfaces 2016;8:7390–5.
[3] Mu Y, Wang N, Sun Z, et al. Carbogenic nanodots derived from organo-templated zeolites with modulated full-color luminescence. Chem. Sci. 2016;7:3564–8.
[4] Zhang JH, Niu A, Li J, et al. In vivo characterization of hair and skin derived carbon quantum dots with high quantum yield as long-term bioprobes in zebrafish. Sci. Rep. 2016;6:37860.
[5] Zhao F, Meng H, Yan L, et al. Nanosurface chemistry and dose govern the bioaccumulation and toxicity of carbon nanotubes, metal nanomaterials and quantum dots in vivo. Sci. Bull. 2015;60:3–20.
[6] Guo Y, Zhang L, Cao F, et al. Thermal treatment of hair for the synthesis of sustainable carbon quantum dots and the applications for sensing Hg^{2+}. Sci. Rep. 2016;6:35795.
[7] Ren X, Ge J, Meng X, et al. Sensitive detection of dopamine and quinone drugs based on the quenching of the fluorescence of carbon dots. Sci. Bull. 2016;61:1615–23.
[8] Zhang J, Dong L, Yu SH. A selective sensor for cyanide ion (CN^-) based on the inner filter effect of metal nanoparticles with photoluminescent carbon dots as the fluorophore. Sci. Bull. 2015;60:785–91.
[9] Jiang Y, Wei G, Zhang W, et al. Solid phase reaction method for preparation of carbon dots and multi-purpose applications. Sens. Actuators B 2016;234:15–20.
[10] Dang H, Huang LK, Zhang Y, et al. Large-scale ultrasonic fabrication of white fluorescent carbon dots. Ind. Eng. Chem. Res. 2016;55:5335–41.
[11] Liu Z, Chen W, Li Y, et al. Integrin $\alpha_v\beta_3$-targeted C-dot nanocomposites as multifunctional agents for cell targeting and photoacoustic imaging of superficial malignant tumors. Anal. Chem. 2016;88:11955–62.
[12] Miao H, Wang L, Zhuo Y, et al. Label-free fluorimetric detection of CEA using carbon dots derived from tomato juice. Biosens. Bioelectron 2016;86:83–9.
[13] Liu ZX, Chen BB, Liu ML, et al. Cu(I)-doped carbon quantum dots with zigzag edge structures for highly efficient catalysis of azide-alkyne cycloadditions. Green Chem. 2017;19:1494–8.
[14] Zhou J, Zhou H, Tang J, et al. Carbon dots doped with heteroatoms for fluorescent bioimaging: a review. Microchim. Acta 2017;184:343–68.
[15] Liu W, Diao H, Chang H, et al. Green synthesis of carbon dots from rose-heart radish and application for Fe^{3+} detection and cell imaging. Sens. Actuators B 2017;241:190–8.
[16] Li H, Shao FQ, Huang H, et al. Eco-friendly and rapid microwave synthesis of green fluorescent graphitic carbon nitride quantum dots for vitro bioimaging. Sens. Actuators B 2016;226:506–11.
[17] Wu Z, Feng M, Chen X, et al. N-dots as a photoluminescent probe for the rapid and selective detection of Hg^{2+} and Ag^+ in aqueous solution. J. Mater. Chem. B 2016;4:2086–9.
[18] Wang M, Zheng B, Yang F, et al. Synthesis of "amphiphilic" carbon dots and their application for the analysis of iodine species (I_2, I^- and IO_3^-) in highly saline water. Analyst 2016;141:2508–14.
[19] Kumar A, Chowdhuri AR, Laha D, et al. Green synthesis of carbon dots from ocimum sanctum for effective fluorescent sensing of Pb^{2+} ions and live cell imaging. Sens. Actuators B 2017;242:679–86.
[20] Pang S, Zhang Y, Wu C, et al. Fluorescent carbon dots sensor for highly sensitive detection of guanine. Sens. Actuators B 2016;222:857–63.
[21] Miao P, Tang Y, Han K, et al. Facile synthesis of carbon nanodots from ethanol and their application in ferric(III) ion assay. J. Mater. Chem. A 2015;3:15068–73.
[22] Li S, Li Y, Cao J, et al. Sulfur-doped graphene quantum dots as a novel fluorescent probe for highly selective and sensitive detection of Fe^{3+}. Anal. Chem. 2014;86:10201–7.
[23] Ali H, Bhunia SK, Dalal C, et al. Red fluorescent carbon nanoparticle-based cell imaging probe. ACS Appl. Mater. Interfaces 2016;8:9305–13.
[24] Wang R, Wang X, Sun Y. Aminophenol-based carbon dots with dual wavelength fluorescence emission for determination of heparin. Microchim. Acta 2017;184:187–93.
[25] Dong Y, Chen Y, You X, et al. High photoluminescent carbon based dots with tunable emission color from orange to green. Nanoscale 2017;9:1028–32.
[26] Liu Y, Zhou L, Li Y, et al. Highly fluorescent nitrogen-doped carbon dots with excellent thermal and photo stability applied as invisible ink for loading important information and anti-counterfeiting. Nanoscale 2017;9:491–6.
[27] Tan J, Zou R, Zhang J, et al. Large-scale synthesis of N-doped carbon quantum dots and their phosphorescence properties in a polyurethane matrix. Nanoscale 2016;8:4742–7.
[28] Wang ZX, Ding SN. One-pot green synthesis of high quantum yield oxygen-doped, nitrogen-rich, photoluminescent polymer carbon nanoribbons as an effective fluorescent sensing platform for sensitive and selective detection of silver(I) and mercury(II) ions. Anal. Chem. 2014;86:7436–45.
[29] Cavicchioli M, Massabni AC, da Costa Ferreira AM, et al. Synthesis, structure and redox properties of an unexpected trinuclear copper(II) complex with aspartame: $[Cu(apm)_2Cu(\mu\text{-N, O:O'-apm})_2(H_2O)Cu(apm)_2(H_2O)]\cdot 5H_2O$. Inorg. Chim. Acta 2005;358:4431–6.
[30] Feng J, Wang WJ, Hai X, et al. Green preparation of nitrogen-doped carbon dots derived from silkworm chrysalis for cell imaging. J. Mater. Chem. B 2016;4:387–93.
[31] Gao ZH, Lin ZZ, Chen XM, et al. Carbon dots-based fluorescent probe for trace Hg^{2+} detection in water sample. Sens. Actuators B 2016;222:965–71.
[32] Edison TN, Atchudan R, Sethuraman MG, et al. Microwave assisted green synthesis of fluorescent N-doped carbon dots: cytotoxicity and bio-imaging applications. J. Photochem. Photobiol. B 2016;161:154–61.
[33] Edison TN, Atchudan R, Shim JJ, et al. Turn-off fluorescence sensor for the detection of ferric ion in water using green synthesized N-doped carbon dots and its bio-imaging. J. Photochem. Photobiol. B 2016;158:235–42.
[34] Huang H, Lv JJ, Zhou DL, et al. One-pot green synthesis of nitrogen-doped carbon nanoparticles as fluorescent probes for mercury ions. RSC Adv. 2013;3:21691–6.
[35] Han Y, Chen Y, Feng J, et al. One-pot synthesis of fluorescent silicon nanoparticles for sensitive and selective determination of 2,4,6-trinitrophenol in aqueous solution. Anal. Chem. 2017;89:3001–8.
[36] Wang Q, Zhang S, Zhong Y, et al. Preparation of yellow-green-emissive carbon dots and their application in constructing a fluorescent turn-on nanoprobe for imaging of selenol in living cells. Anal. Chem. 2017;89:1734–41.
[37] Li L, Liu D, Mao H, et al. Multifunctional solid-state electrochemiluminescence sensing platform based on poly(ethylenimine) capped N-doped carbon dots as novel co-reactant. Biosens. Bioelectron 2017;89:489–95.
[38] Wang ZX, Kong FY, Wang W. Near-ultraviolet fluorescent "on-off-on" switching sensors based on nitrogen-enriched dual-color single-functional polymer carbon nanosheets. Chem. Eur. J. 2017;23:665–75.
[39] Hou J, Wang W, Zhou T, et al. Synthesis and formation mechanistic investigation of nitrogen-doped carbon dots with high quantum yields and yellowish-green fluorescence. Nanoscale 2016;8:11185–93.
[40] Gao F, Ma S, Li J, et al. Rational design of high quality citric acid-derived carbon dots by selecting efficient chemical structure motifs. Carbon 2017;112:131–41.
[41] Liao J, Cheng Z, Zhou L. Nitrogen-doping enhanced fluorescent carbon dots: Green synthesis and their applications for bioimaging and label-free detection of Au^{3+} ions. ACS Sust. Chem. Eng. 2016;4:3053–61.
[42] Zhang HY, Wang Y, Xiao S, et al. Rapid detection of Cr(VI) ions based on cobalt (II)-doped carbon dots. Biosens. Bioelectron 2017;87:46–52.
[43] Mao QX, E S, Xia JM., et al. Hydrophobic carbon nanodots with rapid cell penetrability and tunable photoluminescence behavior for in vitro and in vivo imaging. Langmuir 2016;32:12221–9.
[44] Wen X, Shi L, Wen G, et al. Green and facile synthesis of nitrogen-doped carbon nanodots for multicolor cellular imaging and Co^{2+} sensing in living cells. Sens. Actuators B 2016;235:179–87.
[45] Wang N, Wang Y, Guo T, et al. Green preparation of carbon dots with papaya as carbon source for effective fluorescent sensing of iron(III) and *Escherichia coli*. Biosens. Bioelectron 2016;85:68–75.
[46] Li JY, Liu Y, Shu QW, et al. One-pot hydrothermal synthesis of carbon dots with efficient up- and down-converted photoluminescence for the sensitive detection of morin in a dual-readout assay. Langmuir 2017;33:1043–50.

Please cite this article in press as: Zhang X et al. Facile and large-scale synthesis of green-emitting carbon nanodots from aspartame and the applications for ferric ions sensing and cell imaging. Sci Bull (2017), http://dx.doi.org/10.1016/j.scib.2017.09.004

[47] Cui X, Wang Y, Liu J, et al. Dual functional N- and S-co-doped carbon dots as the sensor for temperature and Fe^{3+} ions. Sens. Actuators B 2017;242:1272–80.
[48] Liu Y, Duan W, Song W, et al. Red emission B, N, S-co-doped carbon dots for colorimetric and fluorescent dual mode detection of Fe^{3+} ions in complex biological fluids and living cells. ACS Appl. Mater. Interfaces 2017;9:12663–72.
[49] Shi B, Su Y, Zhang L, et al. Nitrogen and phosphorus co-doped carbon nanodots as a novel fluorescent probe for highly sensitive detection of Fe^{3+} in human serum and living cells. ACS Appl. Mater. Interfaces 2016;8:10717–25.
[50] Wang C, Jiang K, Wu Q, et al. Green synthesis of red-emitting carbon nanodots as a novel "turn-on" nanothermometer in living cells. Chem. Eur. J. 2016;22:14475–9.
[51] Wu X, Sun S, Wang Y, et al. A fluorescent carbon-dots-based mitochondria-targetable nanoprobe for peroxynitrite sensing in living cells. Biosens. Bioelectron 2017;90:501–7.
[52] Zhang J, Yu SH. Carbon dots: large-scale synthesis, sensing and bioimaging. Mater. Today 2016;19:382–93.

Please cite this article in press as: Zhang X et al. Facile and large-scale synthesis of green-emitting carbon nanodots from aspartame and the applications for ferric ions sensing and cell imaging. Sci Bull (2017), http://dx.doi.org/10.1016/j.scib.2017.09.004